Article

Importance of Topographical Recognition of Pulmonary Arteries in Diagnostics and Treatment of CTEPH, Based on Analysis of a Dissected Case Model – Pilot Study

Matiss Zicans [*] , Dzintra Kazoka , Mara Pilmane , Andris Skride

Article

Importance of Topographical Recognition of Pulmonary Arteries in Diagnostics and Treatment of CTEPH, Based on Analysis of a Dissected Case Model – Pilot Study

Matiss Zicans [1], *, Dzintra Kazoka [2], Mara Pilmane [2] and Andris Skride [3, 4]

[1] Faculty of Medicine, Rīga Stradiņš University, LV-1007 Riga, Latvia; matisszicans@gmail.com (M.Z.)

[2] Institute of Anatomy and Anthropology, Rīga Stradiņš University, LV-1010 Riga, Latvia; Dzintra.Kazoka@rsu.lv (D.K.); Mara.Pilmane@rsu.lv (M.P.)

[3] Department of Internal Diseases, Rīga Stradiņš University, LV-1007 Riga, Latvia; Andris.Skride@rsu.lv (A.S)

[4] Pauls Stradiņš Clinical University Hospital, LV-1002 Riga, Latvia; Andris.Skride@rsu.lv (A.S.)

* Correspondence: matisszicans@gmail.com

Abstract: Background: Knowledge of the anatomy of pulmonary arteries is essential in many invasive procedures concerning pulmonary circulation. In the diagnosis and treatment of chronic thromboembolic pulmonary hypertension (CTEPH), two-dimensional (2D) pulmonary angiography is used. Recognizing the topographic course of the pulmonary arteries and understanding the status in three-dimensions (3D) is paramount. The study aimed to evaluate and describe the branching variant of pulmonary arteries in a single case, as well as morphological parameters of the segmental arteries, like length, diameter and branching angles. Methods: One pair of embalmed human cadaver lungs were dissected by scalpel, surgical forceps and measured until the subsegmental arteries. Results: The diameters (ranging from 3.04 to 9.29 mm) and lengths (ranging from 9.09 to 53.91 mm) of the pulmonary segmental arteries varied. The proximal branching angles were wide and close to perpendicular, while distally, the angles between the segmental and subsegmental arteries were narrower (30-45°). Upon evaluating the branching, rare variations were identified and delineated, notably in the lower lobes of both lungs. Conclusions: Utilizing knowledge and data in clinical settings is instrumental for effectively diagnosing and treating CTEPH. Further research is required to explore the complications in invasive procedures related to various anatomical variations.

Keywords: pulmonary arteries; anatomy; dissection; chronic thromboembolic pulmonary hypertension; angiogram

1. Introduction

The pulmonary circulatory system constitutes an intricate network of blood vessels that is detailed and structured to facilitate the efficient exchange of gases, thereby enabling the delivery of oxygen to the organs and tissues of the human body [1]. Additionally, due to the numerous variations in the arteries, physicians must have a comprehensive knowledge of their anatomy to minimize the risk of adverse intraoperative procedures [2]. Clinicians, surgeons and radiologists must thoroughly understand the normal anatomy of the pulmonary vessels. The branching and typical imaging appearance of the pulmonary arterial tree are crucial for diagnosing and characterizing various pathologies of the pulmonary arteries. The complex variations of blood vessels within the traditional anatomical borders present significant challenges for medical specialists, particularly those specializing in cardiothoracic surgery [3].

The pulmonary trunk originates from the heart's right ventricle and initially moves forward, then to the back and side on the left of the ascending aorta. At the level of the aortic arch, the

pulmonary trunk divides into the right and left pulmonary arteries. The right pulmonary artery passes under the aortic arch and enters the hilum of the right lung in front of the right bronchus. Meanwhile, the left pulmonary artery enters the hilum of the left lung above the left bronchus.

The branching patterns of these blood vessels differ between the lungs due to their anatomical variations, with the most significant variability reported in the branching of segmental and subsegmental arteries [4]. Determination of the branches is an essential aspect when attempting to assess the pulmonary vascular tree. Studying the distribution of flow resistance in the arterial tree of the lung requires a comprehensive analysis of the various quantitative aspects, including the exact numbers and lengths of each branch. This task is particularly challenging due to the irregularity of the arterial tree's structure. Identifying systematic distributed structures introduces complexity that may pose challenges for conventional morphometric research methods.

Various disorders can affect the pulmonary arteries, occasionally incidentally discovered during imaging for other reasons or as part of the work-up for symptomatic patients. Chronic thromboembolic pulmonary hypertension (CTEPH) experiences morphologic changes in the vasculature [5]. It is a rare disease with an annual incidence of 3.1-6.0 and a prevalence – of 25.8-38.4 cases per million [6]. It is diagnosed via invasive pulmonary angiography (PA) combined with right heart catheterization. CTEPH is also one of the pulmonary hypertension (PH) subtypes, representing Group 4 (based on the World Health Organization (WHO) classification) that can potentially be cured [7]. Other groups include pulmonary arterial hypertension (Group 1), pulmonary hypertension associated with left-sided heart failure (Group 2), pulmonary hypertension secondary to lung disease (Group 3), and multifactorial pulmonary hypertension (Group 5). The treatment for CTEPH includes pulmonary endarterectomy ((PEA), class – I, evidence level – B) and/or balloon pulmonary angioplasty ((BPA), class – I, evidence level – B), complimented with drug therapy, if required [8,9]. It is essential to accurately note, label and document the stenotic and occluded lobar and segmental arteries during the diagnostic procedure to ensure the best possible treatment. In treatment via BPA, identical imaging modalities are employed; therefore, explicit preparation, which is essential during diagnostic PA, is crucial. Although the rate of complications in BPA has decreased in past years, it remains high.

The rate of complications related to pulmonary injury varies from 5.9% to 31.4% [10,11], while the early mortality rate is considered to be 0-14%, depending on the experience of the respective CTEPH clinical center [12]. Serious but quite common adverse events include catheter wire-caused vascular injuries, leading to hemoptysis, vascular dissection, and balloon-induced perforation of pulmonary arteries [13]. Older age and higher mean pulmonary artery pressure are often associated with a higher risk of complications [14,15]. Unexpected punctures or perforations might be related to the inability to correctly locate the course of a segmental artery, misunderstanding the bifurcation angles in different planes, or misinterpreting the original diameter of the artery as it courses dorsally.

It is essential to emphasize the significance of anatomical variations and arterial morphology in these complications. Besides, a better understanding of topographical arterial anatomy would allow the invasive specialist to perform the PA and BPA procedures quicker, decreasing the risk of complications and the dose of radiation absorbed.

This study aimed to better understand the pulmonary arteries and their branching using a dissected case and apply this knowledge to the diagnostics and treatment of CTEPH. We focused on the morphological variations of the pulmonary arteries in a cadaveric sample.

2. Materials and Methods

2.1. Study Design

From October 2023 to May 2024, an anatomical assessment of the pulmonary arteries was carried out using a pair of human embalmed cadaver lungs provided by the Laboratory of Anatomy and the Department of Morphology of the Institute of Anatomy and Anthropology of Rīga Stradiņš University. The cadaver was a 93-year-old male with a relatively healthy life status. A relative's consent form was obtained before the cadaver was used for scientific purposes. The study involved

analyzing the branching patterns of the pulmonary arteries and macroscopically observing, studying and photographing the anatomical distributions. The methods and procedures complied with the applicable instructions, guidelines and regulations. Approval from the Research Ethics Committee of Rīga Stradiņš University was received (Ethical approval code: 2-PĒK-4/153/2024).

2.2. Dissection Procedure

The thoracic cavity of the male cadaver, which was fixed with the classical formaldehyde method, was opened first. For this part of the dissection, a method described by Barberini was used [16]. In this region, the skin of the thorax was removed by scalpel, and then sternotomy was performed. A bone saw was used to make a vertical incision through the anterior aspect of the ribs, which were folded back and to both sides, revealing lungs with the heart between them. The pericardium was peeled off, and the lungs were separated from the diaphragm using a scalpel and forceps. To continue the dissection, the lung-heart complex needed to be extracted from the body. The superior and inferior caval veins were cut off at the height of the right atrium, and the ascending aorta was cut off right above the base of the outflow tract. After removing the lungs from the body, the pulmonary trunk was cut off at its base. The heart was separated entirely from the lungs. The bifurcation of the pulmonary trunk was easily visualized.

Further dissection included removing lung parenchyma, bronchi, veins, nerves and preserving only arteries. The principal bronchi and pulmonary veins were cut off straight away to improve the accessibility for the dissection.

The dissection procedure was based on the principle of following the respective pulmonary artery and removing the lung tissue millimeter by millimeter so as not to cut off some arterial branches accidentally. The process started at the hilum of the lung and continued ventrally, laterally and dorsally in the lung periphery. At the segmental level, the bronchi were accompanying arteries, which made it easier to dissect – removing these bronchi was sometimes effortless, revealing a clear path for the partner artery. In the middle of the dissection, for better accessibility at the bifurcation of the pulmonary trunk, the right pulmonary artery was cut off, which resulted in right and left lung separation, and the dissection was continued for the two separate parts. The dissection was stopped after revealing all the segmental and most of the subsegmental arteries, in consideration of the fragility of the lungs and arteries. Red acrylic paint and a small brush were used to paint all the arteries down to the subsegmental level to emphasize the anatomy of the pulmonary arteries.

2.3. Evaluation of the Arterial Branching, Measurements and Comparisons

After the dissection, the branching variant in both lungs was assessed. The non-arterial tissue were removed using forceps and a scalpel to expose the pulmonary arterial branches fully. The recognition of pulmonary segmental arteries is indicated by the letter A, representing the artery, followed by a number corresponding to the pulmonary segments they serve. In cases where two separate arteries supply the same pulmonary segment and do not have a common origin, a lowercase letter (either a or b) is used after the number to denote the subsegmental branch. For example, the anterior segment (S3) is supplied by A3a and A3b.

The identified arterial branches were then measured accordingly. The morphological parameters (length, diameter of each artery and also the angles of bifurcation between the arteries) were detected by plastic ruler, digital caliper and protractor. All these measurements were taken by hand, each distance and angle measured five times and the mean value was taken as the final measurement.

Data from scientific literature (selective search of articles from PubMed, Scopus (published from 1956 to 2024)) were used and analyzed to compare pulmonary artery branching patterns. In search of articles, the following keywords were used: "pulmonary arterial tree", "branching of pulmonary arteries", "morphology and morphometry of pulmonary arteries", and "branching pattern/variations in pulmonary arteries". The articles were selected based on their titles and abstracts, and complete text articles were carefully evaluated with the language requirement of being published in English. Some articles were excluded because the pulmonary arteries were described at a more distal

subsegmental level, including only one lung lobe. The included articles describe the branching of lobar and segmental arteries. For this research, all articles containing detailed descriptions of the morphometry of pulmonary arteries up to the subsegmental branches were included.

Related to segmental arteries' variations, Michaud's approach was rooted in the concept of its description [17], where each lung is divided into ten segmental zones. In the right lung, the bronchopulmonary segments consist of several subunits, including the apical (A1), posterior (A2), anterior (A3), lateral (A4), medial (A5), superior (A6), medial basal (A7), anterior basal (A8), lateral basal (A9) and posterior basal (A10) segments in the right lung. In the left lung, the bronchopulmonary segments include the apicoposterior (A1+2), anterior (A3), superior lingular (A4), inferior lingular (A5), superior (A6), anteromedial basal (A7+8), lateral basal (A9) and posterior basal (A10) segments.
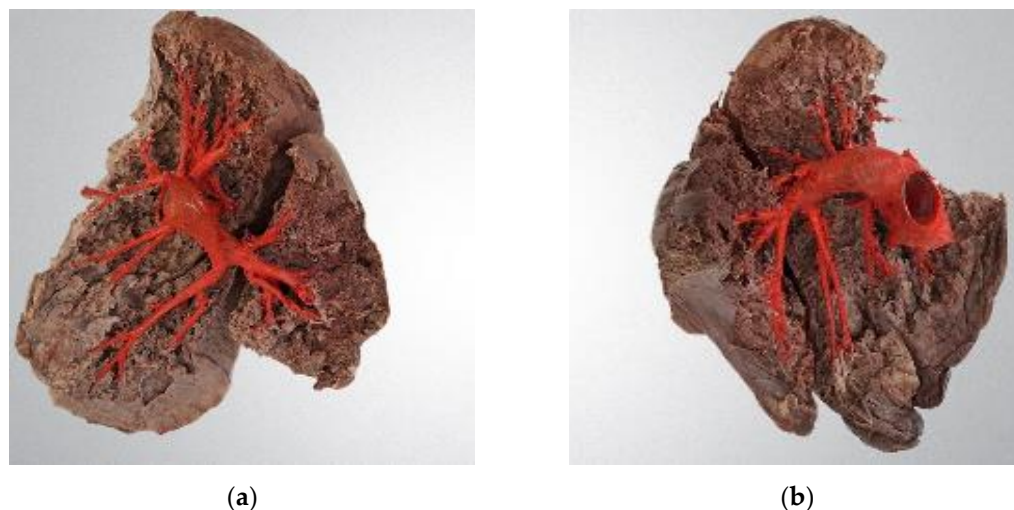
2.4. Statistical Methods

An evaluation of the morphometry of the pulmonary arteries was carried out using Microsoft Excel (2016) to examine the distribution of the data, which was represented through the mean and standard deviation (SD). The coefficient of variation (CV) was computed to compare measurements of different types and units, serving as a statistical indicator of the relative scattering of data points in a data set around an average. Data regarding the length and width of arteries were tabulated, demonstrating the artery's generation and morphometric parameters like length and diameter.

3. Results

The study examined a thorough account of the branching arrangement in a single dissected human sample. Each lung can exhibit as many as ten observable segmental arteries. It also emphasized that the branching configurations of the pulmonary arteries should be regarded as distinct entities on each side and not be compared directly.

Figure 1 presents the result of human cadaver lung dissection to preserve pulmonary arteries and mark them in red. The pulmonary arteries in the left and right lungs form two distinct patterns.
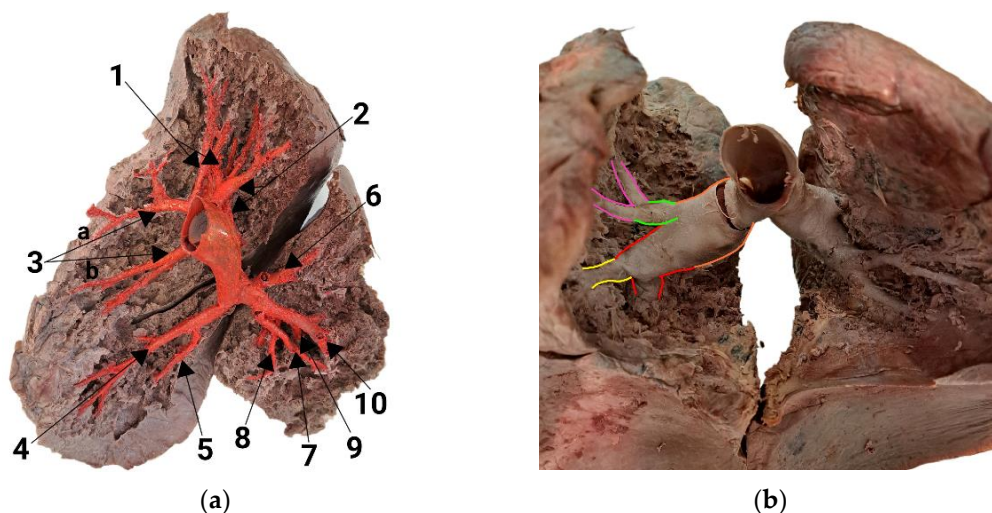

(**a**)   (**b**)

Figure 1. Dissected human lungs: (**a**) Right (on the left); (**b**) Left (on the right). Pulmonary arteries are colored in red; the picture is taken in medial projection.

3.1. Branching Variant of the Right Lung

The anatomical structure and division of the right lung are illustrated in Figure 2 (a) and (b). The right pulmonary artery (RPA) splits into the anterior trunk and interlobar artery after the RPA courses horizontally for a few centimeters. The anterior trunk is frequently observed in the right lung and is more clearly visible in the AP projection, as Figure 2 (b) depicts. It provides most of the upper lobe's blood supply, delivering A1, which supplies the apical segment with numerous subsegmental

branches: A2a, responsible for the posterior segment, and two branches, A3a and A3b, which provide the anterior segment. In the upper lobe, the arteries are very condensed and overlap – this is a prime example of the necessity of the 3-dimensional (3D) model. The interlobar artery then courses caudally and dorsally. The first branch it gives off is A2b, which turns upwards to the posterior segment. So, the upper lobe's three segments are supplied with oxygen-poor blood by the anterior trunk and A2b (posterior segmental artery). The interlobar artery gives rise to additional arteries at the level of the middle lobe. Ventrally, it gives origin to the common trunk of A4 and A5, which subsequently diverge into A4 and A5, supplying the corresponding segments of the middle lobe. A4 follows a more lateral course, while A5 takes a medial trajectory. Opposite to this trunk, A6 courses dorsally supplying the superior segment. The A4+5 trunk branches off at the same level as A6, and the branching angles between the interlobar artery and A4+5 and the interlobar artery and A6 are nearly perpendicular. The interlobar artery terminates in three branches: A7, A8 and a trunk of A9+10. When looking at the arteries from the front, it can be quite challenging to differentiate between these lower lobe arteries. In such situations, a 3D dissected model can be beneficial, just like when examining the apical part of the lung.

In Figure 2 (a), the medial view clarifies the arteries' differentiation. A7 runs towards the viewer, A8 supplies the anterior part of the lower lobe and bifurcates into A9 and A10. A9 extends laterally, while A10 courses posteriorly and medially. The trifurcation of the interlobar artery occurs immediately after it enters the lower lobe, identifiable in Figure 2 (a) due to the prominent fissure between the middle and lower lobes.
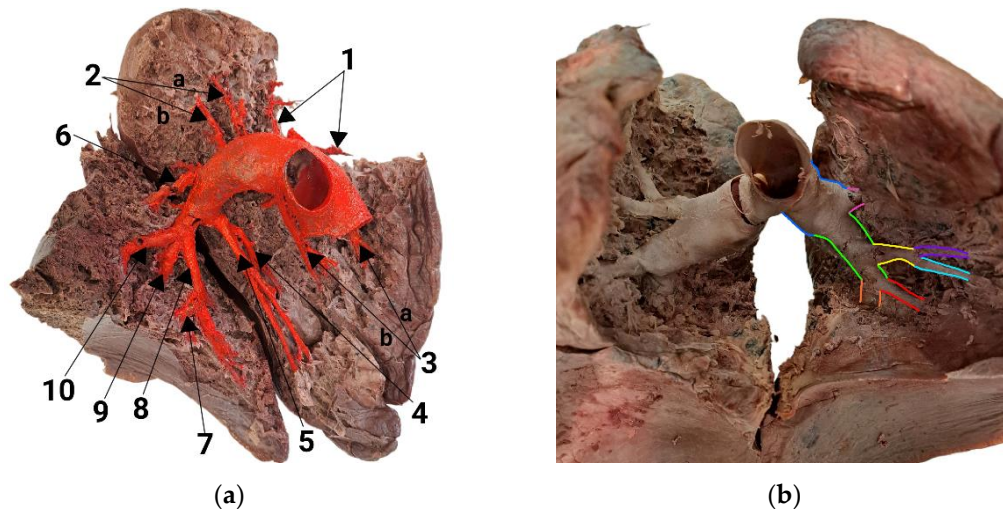

(**a**)   (**b**)

Figure 2. Pulmonary arteries of the right lung: (**a**) Medial view; (**b**) Anterior view. The numbers adjacent to the segmental arteries denote the specific lung segment supplied by each artery: 1 – A1/apical, 2 – A2/posterior, 3 – A3/anterior, 4 – A4/lateral, 5 – A5/medial, 6 – A6/superior, 7 – A7/medial basal, 8 – A8/anterior basal, 9 – A9/lateral basal, 10 – A10/posterior basal. Additionally, different colors represent the arteries: orange – right pulmonary artery; red – interlobar artery; green – anterior trunk; pink – A3/anterior segmental artery; yellow – A4+A5 trunk/trunk of lateral and medial segmental arteries.

3.2. Branching Variant of the Left Lung

In Figure 3 (a) and (b), the pulmonary arteries of the left lung are depicted. Unlike the right lung, there is no anterior trunk present. In this dissection, the upper lobe receives blood from five individual arteries: three arteries supply the apicoposterior (S1,2) segment, and two supply the anterior (S3) segment. After branching off to S1,2 and S3, the left pulmonary artery (LPA) transitions into the interlobar artery. The initial branches of the artery are known as A3a, A3b and A1. These branches further split into smaller arteries, known as subsegmental arteries. The interlobar artery extends downward and toward the back, giving two more separate branches, A2a and A2b, which supply blood to the apicoposterior segment. As it continues downward, the interlobar artery

branches into S4 and S5. A central branch called A4+5 also separates from the interlobar artery towards the front. The common trunk divides into two branches, A4 and A5, with A4 running just above A5. The A6 branches off the interlobar artery and then descends to supply blood to the superior lung segment (S6). The interlobar artery ends in three branches (labeled A8, A9 and A10), which provide blood to S8, S9, and S10, covering the entire basal part of the lung. A8 takes a medial and ventral course and gives rise to a small A7 branch that supplies the reduced or absent medial basal segment (S7). A9 supplies the lateral basal part of the lung and extends posteriorly to A10.

Figure 3. Pulmonary arteries of the left lung: (**a**) Medial view; (**b**) Anterior view. The numbers following the segmental arteries represent the specific segments that each artery supplies, as follows: 1 and 2 – A1,2/apicoposterior, 3 – A3/anterior, 4 – A4/superior lingular, 5 – A5/inferior lingular, 6 – A6/superior, 7 – A7/medial basal, 8 – A8/anterior basal, 9 – A9/lateral basal, 10 – A10/posterior basal. A2a, A2b, A3a, and A3b are pairs of segmental arteries that supply the posterior part of the apicoposterior segment (S1,2) and the anterior segment (S3). The colors representing arteries are as follows: dark blue – left pulmonary artery; green – interlobar artery; pink – A3/anterior segmental artery; yellow – A4+A5 trunk (trunk of superior and inferior lingular arteries); red – A8/anterior basal segmental artery; orange – A10/posterior basal segmental artery; light blue – A5/inferior lingular artery; purple – A4/superior lingular artery.

3.3. Morphological Parameters of the Dissected Model

The study assessed the morphological parameters of pulmonary arteries, examining the length and lumen diameter from the pulmonary trunk to the segmental arteries. The pulmonary trunk was categorized as the first-generation artery. Twenty segmental arteries were included in the analysis. It's important to note that not all segmental arteries are part of the same generation of branching. The study observed that the segmental arteries were primarily of the 3rd and 4th generations, with eight arteries belonging to each category out of the total 20 identified. Additionally, four segmental arteries were classified as the 5th generation.

Tables 1 and 2 detail the arterial development stages for lung segments. The diameters and lengths of these arteries vary widely. The narrowest artery, A8 of the left lung, measures 3.04 mm wide, while the broadest artery, A1 of the right lung, measures 9.29 mm. In terms of length, the shortest artery is A3 of the left lung, measuring 9.09 mm, and the longest is A4 of the right lung, measuring 53.91 mm.

The segmental arteries were analyzed based on their generation rather than being grouped together, which provides a more precise anatomical view. This approach accounts for the size differences among the arteries and offers valuable insights for anatomical studies.

Table 1. The generation, length and diameter of pulmonary arteries in the right lung.

Artery	Generation	Length, mm	Diameter, mm
Pulmonary trunk	1	48.51	29.70
Right pulmonary artery	2	33.15	25.95
A1, apical	3	18.20	9.29
A2, posterior	3	- [2]	5.87
A3, anterior [1]	3	29.82	7.81
A4, lateral	4	53.91	5.63
A5, medial	4	36.84	4.84
A6, superior	3	17.87	7.43
A7, medial basal	4	15.93	4.75
A8, anterior basal	4	16.81	7.20
A9, lateral basal	5	37.68	4.34
A10, posterior basal	5	20.46	6.92

[1] A3 measurements were obtained by averaging the values of A3a and A3b. [2] The length of the A2 artery was indeterminable due to its severance during dissection.

Table 2. The generation, length and diameter of pulmonary arteries in the left lung.

Artery	Generation	Length, mm	Diameter, mm
Pulmonary trunk	1	48.51	29.70
Left pulmonary artery	2	29.46	25.87
A1, apical	3	15.98	4.48
A2, posterior [1]	3	14.77	3.64
A3, anterior [1]	3	9.09	7.48
A4, superior lingular	4	19.34	4.79
A5, inferior lingular	4	15.87	4.76
A6, superior	3	19.09	6.65
A7, medial basal	5	12.02	5.25
A8, anterior basal	5	15.78	3.04
A9, lateral basal	4	11.26	6.33
A10, posterior basal	4	28.94	6.42

[1] Measurements of A2 and A3 were obtained by calculating the mean values of A2a, A2b, A3a and A3b.

The mean length values for each generation of the dissected case are presented in Table 3. In the model, it was observed that contrary to expectations, the 3rd generation arteries were, on average, the shortest. These arteries, which branch off the right and left pulmonary or interlobar arteries, typically act as trunks with a relatively small length-to-width (diameter) ratio. For example, A3b is a 3rd generation artery that appears short but gives rise to long subsegmental branches. Similarly, the common trunk of A4+A5, a 3rd generation artery, bifurcates into longer A4 and A5 – 4th generation arteries.

Table 4 shows the relationship between artery generation and mean diameter. There is a substantial decrease in diameter from the 2nd generation (right and left pulmonary arteries, interlobar arteries) to the 3rd generation arteries, with the subsequent reduction being more gradual. Figure 1 demonstrates how arteries progressively shrink with each bifurcation as they extend distally within the lung.

Tables 3 and 4 present the morphometric analysis of pulmonary arteries, which involves grouping segmental arteries by generation for the most precise comparison. The mean values, standard deviations (SD) and coefficient of variation (CV) are presented.

Table 3. Statistical analysis of arteries' generation and mean length.

Generation	Mean, mm	SD, mm	CV, %
2	31.31	1.85	5.89
3	17.83	5.79	32.47
4	24.86	13.44	54.06
5	21.46	9.82	45.69

Table 4. Statistical analysis of arteries' generation and mean diameter.

Generation	Mean, mm	SD, mm	CV, %
2	25.91	0.04	0.15
3	6.58	1.73	26.29
4	5.59	0.90	16.03
5	4.89	1.41	28.88

In Table 3, the coefficient of variation exceeding 30% indicates significant dispersion in artery lengths within the same generation, potentially misleading mean values. However, Table 4 displays a neater pattern with a coefficient of variation below 30% for all generations (2nd to 5th), providing a more reliable insight into changes in arterial diameters.

Three types of branching angles were measured and compared in a recent study. The first measurements included angles between the interlobar artery and its lateral branches, such as separate segmental arteries and standard trunks (e.g., the trunk of A4+A5). The second set of measurements focused on angles formed by different segmental arteries originating from a single bifurcation, including angles between A4 and A5, A8 and A9, A9 and A10, and the arteries of the upper lobe. Finally, the third set of measurements involved angles formed by bifurcations of the segmental arteries, specifically for all successfully dissected subsegmental arteries. Mean values for each group of angles are presented in Table 5, showcasing the comparative analysis of these branching angles.

Table 5. The branching angles of pulmonary arteries in right and left lungs.

Branching angle group	Mean angle, right lung	Mean angle, left lung
Off the interlobar artery	85.0°	77.0°
Between the segmental arteries	57.5°	38.0°
Between the subsegmental arteries	28.0°	33.6°

The proximal branching angles of the interlobar artery are wide and close to perpendicular, indicating the presence of redundant branches, which are prominent in interlobar artery branching. Dichotomous branching is absent at this point. Moving more distally, the angles between the segmental arteries are closer to 45 degrees, indicating dichotomous branching, with these arteries being similar in size. The most distal angles between the subsegmental arteries are even narrower, close to 30 degrees and exhibit typical dichotomous branching.

4. Discussion

Pulmonary vasculature anatomy varies among patients, including differences in the size and angulation of vessels. It's crucial to accurately differentiate between the pulmonary arteries and veins (A/V) when diagnosing and treating pulmonary conditions [18]. A thorough physical examination can detect around 75% of cases in high-risk populations [19]. Fibrotic transformation of pulmonary artery thromboembolism results in chronic obstruction in the macroscopic pulmonary arteries and vascular remodeling in the microvasculature of the pulmonary system [20]. Pulmonary artery pressure monitors enable remote assessment of cardiopulmonary hemodynamics, allowing for early intervention, and this has been proven to reduce hospitalization due to heart failure [21,22].

Increased peripheral pulmonary vascular resistance can significantly impact cases of pulmonary hypertension (PH) [23]. The right main pulmonary artery runs horizontally in the human body and is presented perpendicular to the right lung. This position creates a right angle with the pulmonary artery trunk, potentially leading to smoother blood flow and increased vulnerability to the effects of PH. On the other hand, the curved trajectory of the left main pulmonary artery may make it comparatively less susceptible to the impact of PH when compared to the right main pulmonary artery. In a study with animals, Harper et al. [24] state that the pulmonary artery is not a source of increased resistance.

A wide range of congenital and acquired conditions can affect the pulmonary arteries, some of which are familiar in clinical practice and others rare. Organized blood clots cause chronic thromboembolic pulmonary hypertension (CTEPH) in the pulmonary arteries. Diagnosing can take 1 to 2 years, which results in higher mortality rates [25,26]. It is recommended that every patient undergoes evaluation at a specialized center with experience in pulmonary arterial endarterectomy (PEA), a potentially curative surgical technique [27]. Patients that are considered inoperable (up to 1/3 of patients) or have blockages in distal parts of the pulmonary arterial tree (segmental and subsegmental arteries) undergo a different type of treatment – balloon pulmonary angioplasty (BPA), which is performed in 2D radiographic control [**28**]. In BPA, knowledge of the topographical anatomy of pulmonary arteries is key to successful treatment via the dilation of narrowed arteries. CTEPH is determined when there is a sustained increase in mean pulmonary artery pressure (at least 20 mm Hg at rest) and evidence of chronic pulmonary embolism on CT, MRI, V/Q scan or PA. A multidetector computed tomography (CT) angiography is typically used to identify indirect (an uneven blood flow pattern in the lungs and the presence of enlarged bronchial arteries) and direct (organized blood clots, partially filled or wholly blocked pulmonary arteries, and thin bands and membranes) signs of CTEPH [9]. Mahammedi et al. [29] found a significant relationship between CT scan measurements of the pulmonary arteries and the severity of PH. MRI is a sensitive and reliable tool for assessing the diagnosis of CTEPH; however, it is rarely used in practice due to the high cost of the examination. V/Q scan is usually performed to rule out CTEPH and diagnose other forms of pulmonary hypertension. It does not reveal specific lobar and segmental arterial branching and precise occlusions, yet it clearly and with high sensitivity demonstrates perfusion defects in lungs that are present in cases of CTEPH.

Diagnosis of CTEPH typically requires invasive pulmonary angiography and right heart catheterization to assess pulmonary arterial pressure [30]. A chronic thromboembolic disease (CTED) diagnosis, distinct from CTEPH, is made if clotting is present without elevated mean pulmonary arterial pressure. As the pulmonary arterial pressures are not determined in CT pulmonary angiography (CTPA), it is not possible to differentiate CTED from CTEPH via CTPA. Besides it is crucial to have a highly experienced radiologist review the CT angiography results, as the test is known to have low sensitivity [31].

The field of PH would greatly benefit from more well-designed studies to improve our understanding of how various conditions contribute to disease development [32]. Evidence has shown that delays in diagnosing and managing CTEPH are associated with poor outcomes [33]. Conventional two-dimensional (2D) imaging-pulmonary angiography may introduce several potential errors when assessing the pulmonary vasculature. However, three-dimensional (3D) chest reconstruction, which involves converting 2D imaging data from CT scans into virtual 3D structures using specialized 3D visualization software, provides a more comprehensive and detailed view of the chest anatomy. Radiography can often reveal enlarged central pulmonary arteries and identify congenital pathology with feasible measurements for clinicians without intravascular contrast material or specialized software [34]. It's important to note that although CT pulmonary angiography (CTPA) is a valuable tool, there are more specific and conclusive methods for diagnosing CTEPH. In routine the first step that leads to the diagnosis of CTEPH is V/Q scan, which is then followed by right heart catheterization and pulmonary angiography to confirm the diagnosis and assess the severity of the disease.

Comprehending the intricate structure and standard imaging features of the pulmonary arterial tree is essential. Pathologies impacting the pulmonary artery can be categorized into five primary groups: congenital conditions, pulmonary artery dilatation, narrowing, filling defects and PH [35]. These conditions are generally identifiable through chest CT or magnetic resonance imaging (MRI). Treatment options exist for almost all variations of this disease [36].

Acquired pulmonary artery variations can lead to different symptoms and expressions. CTEPH often involves the central vasculature, which affects the segmental or subsegmental vessels in other cases. Radiologists and medical specialists should identify vascular differences and communicate their significance to surgeons [37]. During a pulmonary lobectomy, particularly in video-assisted thoracic surgery (VATS), surgeons may encounter technical challenges stemming from variations in the anatomy of the pulmonary arterial tree [38]. Such anatomical diversity can pose complex and intricate obstacles that require careful navigation during the surgical procedure. Performing the intricate dissection, isolation, and closure of the artery branches in a lung lobe to be resected is also one of the most complex steps in a standard pulmonary lobectomy.

Anatomical cadaveric dissections have long been integral to research, significantly enhancing the understanding of vascular anatomy for many years. Only a handful of studies in the existing literature delve into lung dissections focused on preserving arterial trees. In contrast, others concentrate on elucidating the morphology of the tracheobronchial tree [39]. The most common branching variations described superficially in most articles give a basic understanding of pulmonary arterial anatomy by describing the segmental branches of each lobe [40]. Murlimanju et al. [41] observed that the variations were higher in the left than in the right lung. Their study detected variations in 16.1% of the right lungs and 48.2% of the left lungs. George et al. [42] found that 67.69% of right lungs have two pulmonary arteries, whereas 3.07% possess three. Other researchers offer more detailed and well-explained branching variations of a single lobe. There are often described up to 8 different branching variations in a lobe [43–46]. Unfortunately, for this research, it was impossible to combine all these variations as in each of the articles, only a single lobe was described, and the criteria for each author in differentiating segmental arteries may be different. Research performed by Michaud et al. [17], which fully describes both lungs, is quite detailed. It presents up to three branching variations for each lobe or cluster of segments. The most common variations usually represent 70-75% of cases, rarer variants were noted in 14-15%, and the rarest occur in less than 10% of cases.

Advanced technology enables the utilization of specialized software to measure digital vascular parameters. Singhal et al. [47] have developed a technique for organizing these measurements using the Strahler order concept. According to this concept, the most distal arteries are designated 1st order. When two arteries of equal size connect, the resulting artery is categorized as a second-order artery. This classification continues for subsequent connections. Our study adjusted the numbering system due to the inaccessibility of the smallest and most distal arteries. For instance, the pulmonary trunk was considered a 1st generation artery, with its primary branches labeled as 2nd generation, and so on. While this approach has been utilized in prior studies, it may not be as comprehensive as the Strahler-order method [48,49].

First, it is essential to note the branching pattern of the right and left pulmonary arteries. They form two distinct structures that cannot be compared, and assumptions should not be made in cases of low-quality PA. There are segmental differences between the lungs. As the segments are supplied by segmental pulmonary arteries running primarily parallel to segmental bronchi, the venous blood supply differs between the lungs [39]. The dissected case shows some excellent examples. After coursing horizontally for a few centimeters, the right pulmonary artery splits into the anterior trunk and interlobar artery.

In contrast, the left pulmonary artery does not split into two major branches – the anterior trunk is absent. It is a common finding, and the anterior trunk is not recognized as a structure in the left lung [17,40]. In cases where segmental branches, such as S4 and S5, share the exact numbering, it is essential to understand the topography of pulmonary segments. S4 and S5 have different lung positions. Thereby, the course of segmental arteries will be different in both – in the right lung from

the common trunk of A4+A5, where A4 branches off laterally, while A5 – medially; however, in the left lung – A4 branches off superiorly, while A5 – inferiorly. Another reason for not comparing the two branching patterns is apparent in the dissected case. The interlobar artery terminates in a trifurcation in both lungs, exhibiting a bilaterally symmetrical pattern. However, these three end branches are not the same in both lungs. In the right lung were A7, A8 and the trunk of A9+10, but in the left – A8, A9 and A10. The dissected model determined that the revealed subsegmental arteries course to the location of each pulmonary segment. However, this may cause difficulties in reading PAs, especially if they are done in only one projection. It could lead to an imprecise diagnosis and a higher probability of complications during procedures.

As conventional pulmonary angiography is a 2D picturing examination, many factors can contribute to an inaccurate reading of the angiogram. Often, the arteries overlap, and it might be challenging to differentiate them, especially in the lower lobes of the lungs. Besides, many branching variations are recorded – up to 8 in each lobe [17,28,43–46]. A few rare variations were recorded in the dissected case based on Michaud's representation. Most commonly, the interlobar artery in both lungs ends in bifurcation – in the right – in A7+A8 and A9+A10, while in the left – in A8 and A10+A9. In our case, trifurcations, as mentioned above, were noted. Also, although the anterior trunk is a common finding in the upper lobe of the right lung, it can be absent [17]. Furthermore, for patients with severe CTEPH and thromboembolic blockages, low cardiac output and inability to hold their breath for a few seconds, the quality of pulmonary angiogram can be deficient. In such situations, the invasive specialist must be aware of the possible anatomical variations and differences in the course of the arteries in these variations. 3D models could be a helpful tool for studying the possible variations, differentiating the segmental arteries and looking at different artery courses in other models. Acquiring data from CT pulmonary angiography is another option for a comprehensive study of 3D anatomy. However, a tangible dissected case represents the most accurate variant of human pulmonary arteries with a size ratio 1:1.

The importance of morphological parameters in diagnosis, pathophysiology, and treatment is not much described in the literature. There is some proof of dysregulation in endothelial cells when the shear stress on the vessel wall in pulmonary arteries is present [50]. Shear stress can also be caused by unusual branching patterns in the pulmonary vasculature. It is not yet known what angles and in which lobes of the lungs would be predisposed to CTEPH due to shear stress (or maybe other factors). However, if systematic evaluation of each pulmonary angiography was performed, some conclusions could be drawn – that is the aim for future studies. Abbasi et al. [51] discovered that there is a significant decrease in the primary pulmonary artery bifurcation angle in patients developing CTEPH.

The branching angles have their role in complications in diagnosing, treating CTEPH and right heart catheterization when the catheter is directed through the pulmonary arteries. Complications include hemoptysis, pulmonary artery perforation and pulmonary artery injury [10,13,15,52]. While specific causes for the injuries are not extensively outlined, unforeseen angling of the pulmonary arteries could be one of the contributing factors. Our results show that some branches of the interlobar arteries form angles close to 90 degrees. As the anatomy course changes direction to almost perpendicular, there is an increased risk of vascular injury when the catheter is inserted into the vessel wall. No evidence has been established regarding the relationship between the angle and complications. However, the invasive specialist should always exercise caution when directing the catheter into the pulmonary arteries. Further research is needed to investigate the complication rate and variations in pulmonary arterial anatomy.

The invasive specialist performing PA and balloon pulmonary angioplasty (BPA) must also be aware of differences in the sizes of pulmonary segmental arteries. Our study showed a vast difference in the diameters of the segmental arteries (3.04-9.29 mm). Other authors have noted quite an extensive variety in segmental arteries' diameters [47,49]. During BPA, the narrowed segmental artery is expanded by inflating a balloon. The specialist performing the procedure must be conscientious as the segmental arteries, especially having fibrotic/thromboembolic material in their wall, are very fragile and can perforate [15]. As the risk of perforation is high, each specialist must know the

differences in morphology of segmental arteries and treat each stenotic or occluded artery separately by not overestimating its original diameter. Improved knowledge and studying of pulmonary arterial morphology might enhance the quality of the provided treatment and decrease the rate of complications.

Summing up the knowledge from the dissected material and other authors' work in describing pulmonary arterial tree anatomy [17,40,43–46,53,54], a detailed sketch of the pulmonary arterial tree was meticulously rendered, showcasing intricate and accurate details. The sketch is now used in clinical practice to document precise CTEPH diagnosis by labeling the stenotic or occluded arteries. After the initial PA assessment, the invasive cardiologist identifies and marks the affected arteries. A sketch of the marked arteries is placed in the patient's medical records for reference in devising further treatment and evaluating the patient's case. That could be a great practice in every hospital for convenient documentation of the disease's diagnosis and/or progression. Furthermore, this approach allows for a systematic review of the CTEPH phenotype, identifying the most affected and less commonly affected arteries. That would allow us to do further research on the pathophysiology and risk factors of CTEPH and review already pronounced hypotheses, e.g., about thromboembolic material forming more prominently in the arteries of the right lung [55].

The study also has certain limitations that should be considered. One obstacle is that the natural variations in human anatomy can lead to unpredictability in the results. Tracing pulmonary artery branching at the macroscopic level through intrapulmonary tissue may have limited our understanding of microscopic branching patterns. Another limitation is that we only had access to a single sample of two lungs, preventing us from conducting a comparative analysis. The dissection procedure was also time-consuming. Furthermore, using preserved, embalmed tissues may not accurately replicate the conditions of live situations. The manual revision of the vascular system and the delicate measuring processes may also risk damaging smaller vessels if not performed with maximal care. There are numerous branching variations, so reviewing a single case does not explain all possible variants. The various morphologies of pulmonary arteries are generally not linked to the pathophysiology of several pulmonary diseases, including CTEPH. Consequently, limited research has been dedicated to this area, resulting in a scarcity of detailed information on pulmonary arterial anatomical morphology. The lack of literature on dissected cadaveric pulmonary arteries and their branching patterns further limits the ability to compare our results with those of other studies. Developing an effective system for processing and interpreting the data becomes a paramount concern in light of these complexities, demanding a detailed and comprehensive approach. More extensive research is needed to understand the variations in the population fully.

5. Conclusions

Study findings show that interventions in the pulmonary arteries can be challenging due to the high degree of anatomical variability and segmental arteries varying in number, size and origin location. Despite some segments' similarities and identical names, the branching pattern of the pulmonary arteries differed between the two observed lungs. Identifying the pulmonary segmental arteries for diagnostic purposes can be significantly improved by having topographic recognition of the branching. Knowing which branches supply which segments in each lung is essential, especially in low-quality imaging or in cases of overlapping of the arteries. The 3D model, when stated next to 2D pulmonary angiographies acquired during diagnosis of CTEPH, allows interpretation of them to be much more accessible, improving the diagnosis's accuracy and the treatment's effectiveness and safety.

Author Contributions: conceptualization, M.Z.; methodology, M.Z. and D.K.; software, M.Z.; validation, M.Z., D.K. and A.S.; formal analysis, M.Z.; investigation, M.Z.; resources, D.K. and A.S.; writing—original draft preparation, M.Z. and D.K.; writing—review and editing, M.Z., D.K., M.P., and A.S.; visualization, M.Z.; supervision, D.K. All authors have read and agreed to the published version of the manuscript.

Informed Consent Statement: Not applicable.

Conflicts of Interest: The authors declare no conflict of interest.

References

1. Aggarwal, V.; Giri, J.; Visovatti, S.H.; Mahmud, E.; Matsubara, H.; Madani, M.; Rogers, F.; Gopalan, D.; Rosenfield, K.; McLaughlin, V.V.; et al. Status and Future Directions for Balloon Pulmonary Angioplasty in Chronic Thromboembolic Pulmonary Disease With and Without Pulmonary Hypertension: A Scientific Statement From the American Heart Association. *Circulation* **2024**, *149*, doi:10.1161/CIR.0000000000001197.
2. Cory, R.A.S.; Valentine, E.J. Varying Patterns of the Lobar Branches of the Pulmonary Artery: A Study of 524 Lungs and Lobes Seen at Operation on 426 Patients. *Thorax* **1959**, 14, 267–280, doi:10.1136/thx.14.4.267.
3. Wąsik, J.; Tubbs, R.S.; Zielinska, N.; Karauda, P.; Olewnik, Ł. Lung Segments from Anatomy to Surgery. *Folia Morphol* **2024**, *83*, 20–34, doi:10.5603/FM.a2023.0011.
4. Armitage, M.N.; Mughal, A.Z.; Huntley, C.C.; Lasserson, D.; Newnham, M. A Multicentre Observational Study of the Prevalence, Management, and Outcomes of Subsegmental Pulmonary Embolism. *J Thromb Thrombolysis* **2023**, *55*, 126–133, doi:10.1007/s11239-022-02714-5.
5. Rahaghi, F.N.; Ross, J.C.; Agarwal, M.; González, G.; Come, C.E.; Diaz, A.A.; Vegas-Sánchez-Ferrero, G.; Hunsaker, A.; Estépar, R.S.J.; Waxman, A.B.; et al. Pulmonary Vascular Morphology as an Imaging Biomarker in Chronic Thromboembolic Pulmonary Hypertension. *Pulm. circ.* **2016**, *6*, 70–81, doi:10.1086/685081.
6. Leber, L.; Beaudet, A.; Muller, A. Epidemiology of Pulmonary Arterial Hypertension and Chronic Thromboembolic Pulmonary Hypertension: Identification of the Most Accurate Estimates from a Systematic Literature Review. *Pulm. circ.* **2021**, *11*, 1–12, doi:10.1177/2045894020977300.
7. Rose-Jones, L.J.; Mclaughlin, V.V. Pulmonary Hypertension: Types and Treatments. *Curr Cardiol Rev* **2015**, *11*, 73–79, doi:10.2174/1573403X09666131117164122.
8. Humbert, M.; Kovacs, G.; Hoeper, M.M.; Badagliacca, R.; Berger, R.M.F.; Brida, M.; Carlsen, J.; Coats, A.J.S.; Escribano-Subias, P.; Ferrari, P.; et al. 2022 ESC/ERS Guidelines for the Diagnosis and Treatment of Pulmonary Hypertension. *Eur Heart J* **2022**, *43*, 3618–3731, doi:10.1093/eurheartj/ehac237.
9. Hoeper, M.M.; Madani, M.M.; Nakanishi, N.; Meyer, B.; Cebotari, S.; Rubin, L.J. Chronic Thromboembolic Pulmonary Hypertension. *Lancet Respir Med* **2014**, *2*, 573–582, doi:10.1016/S2213-2600(14)70089-X.
10. Brenot, P.; Jaïs, X.; Taniguchi, Y.; Garcia Alonso, C.; Gerardin, B.; Mussot, S.; Mercier, O.; Fabre, D.; Parent, F.; Jevnikar, M.; et al. French Experience of Balloon Pulmonary Angioplasty for Chronic Thromboembolic Pulmonary Hypertension. *Eur Respir J* **2019**, *53*, doi:10.1183/13993003.02095-2018.
11. Wiedenroth, C.B.; Deissner, H.; Adameit, M.S.D.; Kriechbaum, S.D.; Ghofrani, H.-A.; Breithecker, A.; Haas, M.; Roller, F.; Rolf, A.; Hamm, C.W.; et al. Complications of Balloon Pulmonary Angioplasty for Inoperable Chronic Thromboembolic Pulmonary Hypertension: Impact on the Outcome. *J Heart Lung Transplant* **2022**, *41*, 1086–1094, doi:10.1016/j.healun.2022.05.002.
12. Tanabe, N.; Kawakami, T.; Satoh, T.; Matsubara, H.; Nakanishi, N.; Ogino, H.; Tamura, Y.; Tsujino, I.; Ogawa, A.; Sakao, S.; et al. Balloon Pulmonary Angioplasty for Chronic Thromboembolic Pulmonary Hypertension: A Systematic Review. *Respir Investig* **2018**, *56*, 332–341, doi:10.1016/j.resinv.2018.03.004.
13. Pereira, A.R.; Cale, R.; Ferreira, F.; Alegria, S.; Sebaiti, D.; Martinho, M.; Repolho, D.; Vitorino, S.; Santos, P.; Loureiro, M.J.; et al. Complications of Balloon Pulmonary Angioplasty for Chronic Thromboembolic Pulmonary Disease According to the Classification Proposed by the 6th World Symposium on Pulmonary Hypertension. *Eur Heart J* **2021**, *42*, ehab724.1916, doi:10.1093/eurheartj/ehab724.1916.
14. Lang, I.; Meyer, B.C.; Ogo, T.; Matsubara, H.; Kurzyna, M.; Ghofrani, H.-A.; Mayer, E.; Brenot, P. Balloon Pulmonary Angioplasty in Chronic Thromboembolic Pulmonary Hypertension. *Eur Respir Rev* **2017**, *26*, 160119, doi:10.1183/16000617.0119-2016.
15. Ito, R.; Yamashita, J.; Ikeda, S.; Nakajima, Y.; Kasahara, T.; Sasaki, Y.; Suzuki, S.; Takahashi, L.; Komatsu, I.; Murata, N.; et al. Predictors of Procedural Complications in Balloon Pulmonary Angioplasty for Chronic Thromboembolic Pulmonary Hypertension. *J Cardiol* **2023**, *82*, 497–503, doi:10.1016/j.jjcc.2023.06.011.
16. Barberini, F.; Brunone, F.A. A "conservative" method of thoracic wall dissection: a proposal for teaching human anatomy. *Ital J Anat Embryol* **2008**, *113*, 187–195.
17. Michaud, E.; Pan, M.; Lakhter, V.; Reddy Maligireddy, A.; Hyder, S.N.; Patel, N.; Moles, V.M.; McLaughlin, V.V.; Agarwal, P.P.; Visovatti, S.H.; et al. Anatomical Variations in Pulmonary Arterial Branches in Patients Undergoing Evaluation for Chronic Thromboembolic Pulmonary Hypertension. *JSCAI* **2023**, *2*, 101108, doi:10.1016/j.jscai.2023.101108.
18. Zhou, Q.; Tan, W.; Li, Q.; Li, B.; Zhou, L.; Liu, X.; Yang, J.; Zhao, D. A New Segment Method for Pulmonary Artery and Vein. *Health Inf Sci Syst* **2023**, *11*, 47, doi:10.1007/s13755-023-00245-8.
19. Tellapuri, S.; Park, H.S.; Kalva, S.P. Pulmonary Arteriovenous Malformations. *Int J Cardiovasc Imaging* **2019**, *35*, 1421–1428, doi:10.1007/s10554-018-1479-x.

20. Chong, C.; Tay, E.; Sia, C.; Poh, K. Chronic Thromboembolic Pulmonary Hypertension: A Review. *smedj* **2021**, 318–325, doi:10.11622/smedj.2021089.

21. Zafar, H.; Neelam-Naganathan, D.; Middleton, J.T.; Binmahfooz, S.K.; Battersby, C.; Rogers, D.; Swift, A.J.; Rothman, A.M.K. Anatomical Characterization of Pulmonary Artery and Implications to Pulmonary Artery Pressure Monitor Implantation. *Sci Rep* **2023**, *13*, 20528, doi:10.1038/s41598-023-47612-9.

22. Yang, J.; Madani, M.M.; Mahmud, E.; Kim, N.H. Evaluation and Management of Chronic Thromboembolic Pulmonary Hypertension. *CHEST* **2023**, *164*, 490–502, doi:10.1016/j.chest.2023.03.029.

23. Koike, H.; Nishimura, T.; Morikawa, M. Quantitative Evaluation of Pulmonary Hypertension Using 4D Flow MRI: A Retrospective Study. *Heliyon* **2024**, *10*, e31177, doi:10.1016/j.heliyon.2024.e31177.

24. Harper, D.D.; Alpard, S.K.; Deyo, D.J.; Lick, S.D.; Traber, D.L.; Zwischenberger, J.B. Anatomic Study of the Pulmonary Artery as a Conduit for an Artificial Lung: *ASAIO J* **2001**, *47*, 34–36, doi:10.1097/00002480-200101000-00009.

25. Zhai, Z.; Boon, G.J.A.M.; Staring, M.; Van Dam, L.F.; Kroft, L.J.M.; Hernández Girón, I.; Ninaber, M.K.; Bogaard, H.J.; Meijboom, L.J.; Vonk Noordegraaf, A.; et al. Automated Quantification of the Pulmonary Vasculature in Pulmonary Embolism and Chronic Thromboembolic Pulmonary Hypertension. *Pulm. circ.* **2023**, *13*, e12223, doi:10.1002/pul2.12223.

26. Ikeda, N. Balloon Pulmonary Angioplasty for Chronic Thromboembolic Pulmonary Hypertension. *Cardiovasc Interv and Ther* **2020**, *35*, 130–141, doi:10.1007/s12928-019-00637-2.

27. Stricker, H. Chronic Thromboembolic Pulmonary Hypertension - a Diagnostic and Therapeutic Update. *Vasa* **2016**, *45*, 195–199, doi:10.1024/0301-1526/a000525.

28. Yang, J.Z.; Poch, D.S.; Ang, L.; Mahmud, E.; Kim, N.H. Balloon Pulmonary Angioplasty in the Current Era of CTEPH Treatment: How Did We Get Here? *Pulm. circ.* **2023**, *13*, e12312, doi:10.1002/pul2.12312.

29. Mahammedi, A.; Oshmyansky, A.; Hassoun, P.M.; Thiemann, D.R.; Siegelman, S.S. Pulmonary Artery Measurements in Pulmonary Hypertension: The Role of Computed Tomography. *J Thorac Imaging* **2013**, *28*, 96–103, doi:10.1097/RTI.0b013e318271c2eb.

30. Robbins, I.M.; Pugh, M.E.; Hemnes, A.R. Update on Chronic Thromboembolic Pulmonary Hypertension. *Trends Cardiovasc. Med.* **2017**, *27*, 29–37, doi:10.1016/j.tcm.2016.05.010.

31. Tunariu, N.; Gibbs, S.J.R.; Win, Z.; Gin-Sing, W.; Graham, A.; Gishen, P.; AL-Nahhas, A. Ventilation–Perfusion Scintigraphy Is More Sensitive than Multidetector CTPA in Detecting Chronic Thromboembolic Pulmonary Disease as a Treatable Cause of Pulmonary Hypertension. *J. Nucl. Med.* **2007**, *48*, 680–684, doi:10.2967/jnumed.106.039438.

32. Simonneau, G.; Montani, D.; Celermajer, D.S.; Denton, C.P.; Gatzoulis, M.A.; Krowka, M.; Williams, P.G.; Souza, R. Haemodynamic Definitions and Updated Clinical Classification of Pulmonary Hypertension. *Eur Respir J* **2019**, *53*, 1801913, doi:10.1183/13993003.01913-2018.

33. Teerapuncharoen, K.; Bag, R. Chronic Thromboembolic Pulmonary Hypertension. *Lung* **2022**, *200*, 283–299, doi:10.1007/s00408-022-00539-w.

34. Shin, S.; King, C.S.; Brown, A.W.; Albano, M.C.; Atkins, M.; Sheridan, M.J.; Ahmad, S.; Newton, K.M.; Weir, N.; Shlobin, O.A.; et al. Pulmonary Artery Size as a Predictor of Pulmonary Hypertension and Outcomes in Patients with Chronic Obstructive Pulmonary Disease. *Respir Med* **2014**, *108*, 1626–1632, doi:10.1016/j.rmed.2014.08.009.

35. Cortopassi, I.O.; Gosangi, B.; Asch, D.; Bader, A.S.; Gange, C.P.; Rubinowitz, A.N. Diseases of the Pulmonary Arteries: Imaging Appearances and Pearls. *Clin Imaging* **2022**, *91*, 111–125, doi:10.1016/j.clinimag.2022.08.018.

36. Olsson, K.M.; Meyer, B.; Hinrichs, J.; Vogel-Claussen, J.; Hoeper, M.M.; Cebotari, S. Chronic Thromboembolic Pulmonary Hypertension. *Dtsch Arztebl Int* **2014**, doi:10.3238/arztebl.2014.0856.

37. Carter, B.W.; Lichtenberger, J.P.; Wu, C.C. Acquired Abnormalities of the Pulmonary Arteries. *Am J Roentgenol* **2014**, *202*, W415–W421, doi:10.2214/AJR.13.11760.

38. Fourdrain, A.; De Dominicis, F.; Blanchard, C.; Iquille, J.; Lafitte, S.; Beuvry, P.-L.; Michel, D.; Merlusca, G.; Havet, E.; Berna, P. Three-Dimensional CT Angiography of Anatomic Variations in the Pulmonary Arterial Tree. *Surg Radiol Anat* **2018**, *40*, 45–53, doi:10.1007/s00276-017-1914-z.

39. Akdeniz, A.; Kara, E. Determining Tracheobronchial Tree with Anatomical Dissection: 204 Cases. *Turk Thorac J* **2021**, *22*, 124–129, doi:10.5152/TurkThoracJ.2021.18111.

40. Kandathil, A.; Chamarthy, M. Pulmonary Vascular Anatomy & Anatomical Variants. *Cardiovasc. Diagn. Ther.* **2018**, *8*, 201–207, doi:10.21037/cdt.2018.01.04.

41. Murlimanju, B.V.; Massand, A.; Madhyastha, S.; Pai, M.M.; Prabhu, L.V.; Saralaya, V.V. Anatomical Variations of the Arrangement of Structures at the Pulmonary Hilum: A Cadaveric Study. *Surg Radiol Anat* **2017**, *39*, 51–56, doi:10.1007/s00276-016-1716-8.

42. George, B.M.; Nayak, S.B.; Marpalli, S. Morphological Variations of the Lungs: A Study Conducted on Indian Cadavers. *Anat Cell Biol* **2014**, *47*, 253, doi:10.5115/acb.2014.47.4.253.

43. Chen, Z.; Chu, X.; Zhang, J.; Fu, R.; Kang, J.; Chen, J.; Jiang, B.; Wu, Y.; Zhong, W.; Nie, Q. The Regularity of Anatomical Variations of Dominant Pulmonary Segments in the Right Upper Lobe. *Thorac Cancer* **2023**, *14*, 462–469, doi:10.1111/1759-7714.14763.

44. Nagashima, T.; Shimizu, K.; Ohtaki, Y.; Obayashi, K.; Kakegawa, S.; Nakazawa, S.; Kamiyoshihara, M.; Igai, H.; Takeyoshi, I. An Analysis of Variations in the Bronchovascular Pattern of the Right Upper Lobe Using Three-Dimensional CT Angiography and Bronchography. *Gen Thorac Cardiovasc Surg* **2015**, *63*, 354–360, doi:10.1007/s11748-015-0531-1.

45. Fan, K.; Feng, J.; Li, Y.; Liu, B.; Tao, R.; Wang, Z.; Zhao, H.; Zhang, Y.; Wang, J.; Zhang, G. Application of Three-dimensional Reconstruction of Left Upper Lung Lobes in Anatomical Segmental Resection. *Thorac Cancer* **2022**, *13*, 1176–1183, doi:10.1111/1759-7714.14379.

46. Barrett, R.J.; Day, J.C.; Tuttle, Wm.M. The Arterial Distribution to the Left Upper Pulmonary Lobe. *J Thorac Surg* **1956**, *32*, 190–197, doi:10.1016/S0096-5588(20)30413-X.

47. Singhal, S.; Henderson, R.; Horsfield, K.; Harding, K.; Cumming, G. Morphometry of the Human Pulmonary Arterial Tree. *Circ Res* **1973**, *33*, 190–197, doi:10.1161/01.RES.33.2.190.

48. Horsfield, K. Axial Pathways Compared with Complete Data in Morphological Studies of the Lung. *Respir Physiol* **1984**, *55*, 317–324, doi:10.1016/0034-5687(84)90054-9.

49. Huang, W.; Yen, R.T.; McLaurine, M.; Bledsoe, G. Morphometry of the Human Pulmonary Vasculature. *J Appl Physiol* **1996**, *81*, 2123–2133, doi:10.1152/jappl.1996.81.5.2123.

50. Salibe-Filho, W.; Araujo, T.L.S.; Melo, E.G.; Coimbra, L.B.C.T.; Lapa, M.S.; Acencio, M.M.P.; Freitas-Filho, O.; Capelozzi, V.L.; Teixeira, L.R.; Fernandes, C.J.C.S.; et al. Shear Stress-Exposed Pulmonary Artery Endothelial Cells Fail to Upregulate HSP70 in Chronic Thromboembolic Pulmonary Hypertension. *PLOS ONE* **2020**, *15*, e0242960, doi:10.1371/journal.pone.0242960.

51. Abbasi, B.; Darvish, A.; Akhavan, R.; Masoud Pezeshki Rad; Farrokh, D.; Emadzadeh, M.; Dehghani, S. Decreased Pulmonary Artery Bifurcation Angle: A Novel Imaging Criterion for the Diagnosis of Chronic Pulmonary Thromboembolism. *Iran J Med Sci.* **2022**, *47*, 360–366, doi:10.30476/IJMS.2021.88058.1926.

52. Velázquez, M.; Maneiro, N.; Albarrán, A.; Sarnago, F.; Huertas, S.; Cruz-Utrilla, A.; Hinojosa, W.; López-Gude, M.J.; Alonso, S.; Revilla, Y.; et al. Balloon Pulmonary Angioplasty Can Be an Effective and Safe Therapeutic Option in Non-Surgical Elderly Patients. *Front. Cardiovasc. Med.* **2022**, *9*, doi:10.3389/fcvm.2022.1001518.

53. Velázquez, M.; Maneiro, N.; Lareo, A.; Albarrán, A.; Huertas, S.; Olazábal, A.P.; Delgado, J.F.; Alonso, S.; Sarnago, F.; García Tejada, J.; et al. Selective Segmental Pulmonary Angiography: Anatomical, Technical and Safety Aspects of a Must-Learn Technique in Times of Balloon Pulmonary Angioplasty for Chronic Thromboembolic Pulmonary Hypertension. *JCM* **2021**, *10*, 3358, doi:10.3390/jcm10153358.

54. Xie, Z.; Zhu, X.; Li, F.; Zhao, J.; Li, C. Pulmonary Arterial Anatomical Patterns: A Classification Scheme Based on Lobectomy and 3D-CTBA. *Thorac Cardiovasc Surg* **2024**, *May 2*, doi:10.1055/s-0044-1786195.

55. Narechania, S.; Renapurkar, R.; Heresi, G.A. Mimickers of Chronic Thromboembolic Pulmonary Hypertension on Imaging Tests: A Review. *Pulm. circ.* **2020**, *10*, 1–17, doi:10.1177/2045894019882620.